2022 IEEE 61st Conference on Decision and Control (CDC)
December 6-9, 2022. Cancún, Mexico

A Barrier-Certified Optimal Coordination Framework for Connected and Automated Vehicles

Behdad Chalaki, *IEEE Student Member*, Andreas A. Malikopoulos, *IEEE Senior Member*

2022 IEEE 61st Conference on Decision and Control (CDC) | 978-1-6654-6761-2/22/$31.00 ©2022 IEEE | DOI: 10.1109/CDC51059.2022.9992572

Abstract— **In this paper, we extend a framework that we developed earlier for coordination of connected and automated vehicles (CAVs) at a signal-free intersection by integrating a safety layer using control barrier functions. First, in our motion planning module, each CAV computes the optimal control trajectory using simple vehicle dynamics. The trajectory does not make any of the state, control, and safety constraints active. A vehicle-level tracking controller employs a combined feedforward-feedback control law to track the resulting optimal trajectory from the motion planning module. Then, a barrier-certificate module, acting as a middle layer between the vehicle-level tracking controller and physical vehicle, receives the control law from the vehicle-level tracking controller and using realistic vehicle dynamics ensures that none of the state, control, and safety constraints becomes active. The latter is achieved through a quadratic program, which can be solved efficiently in real time. We demonstrate the effectiveness of our extended framework through a numerical simulation.**

I. Introduction

The influential work of Athans [1] on safely coordinating CAVs at merging roadways generated significant interest in this area. Several research efforts since then have considered a two-level optimization framework. This framework includes an *upper-level* optimization that yields, for each CAV, the optimal time to exit the control zone combined with a *low-level* optimization that yields for the CAV the optimal control input (acceleration/deceleration) to achieve the optimal time derived in the upper level subject to the state and control constraints. There have been several approaches in the literature to solve the upper-level optimization problem [2]–[7]. Given the solution of the upper-level optimization problem, a constrained optimal control problem is solved sequentially in the low-level optimization providing the optimal control input for each CAV. To address the low-level optimization problem, research efforts have used optimal control techniques [8]–[12], which yield closed-form solutions, and model predictive control [5], [13]–[15].

Other approaches in the literature have explored the idea of employing control barrier functions (CBF) to ensure the satisfaction of constraints in a safety-critical system. Ames et al. [16] presented a framework to unify safety constraints along with performance objectives of safety-critical system with affine control using CBFs and the control Lyapunov functions (CLFs), respectively. Under reasonable assumptions, they proved that CBF provides a necessary and sufficient condition on the forward invariance of a safe set. A comprehensive discussion of the recent effort on CBFs and their use to verify and enforce safety in the context of safety-critical controllers is provided in [17].

More recently, there have been a series of papers initially proposed by Xiao et al. [18], [19] on using CBFs in the coordination of CAVs [18]–[22]. Xiao et al. [19], provided a joint CBF and CLF approach to respond to inevitable perturbation and noise in a highway merging problem. Focusing on the highway merging problem in [18], the authors presented their two-step approach. First, using linearized dynamic and quadratic costs, they derived the unconstrained solution to the optimal control problem. Next, by formulating a QP at each time step, they tracked the optimal control trajectory using CLF and ensured the satisfaction of the constraints through CBF constraints. Khaled et al. [21] applied the formulation in [19] to a signal-free intersection, while Rodriguez and Fathi [20] employed the two-step formulation in [18] to a signalized intersection.

In this paper, we build upon the framework introduced in [10] consisting of a single optimization level aimed at both minimizing energy consumption and improving the traffic throughput. Utilizing the proposed framework, each CAV computes the optimal unconstrained control trajectory without activating any of the state, control, and safety constraints. One direct benefit of this framework is that it avoids the inherent implementation challenges in solving a constrained optimal control problem in real time. For cases where deviations between the actual trajectory and the planned trajectory exist, some constraints of the system may become active. To address this issue, one approach is to employ a replanning mechanism [23] which introduces an indirect feedback in the system. Another approach is to consider learning these deviations and uncertainties online [24]. Using CBF for safety-critical systems [16], we integrate a safety layer into our framework to guarantee that the planned trajectory does not violate any of the constraints in the system. Particularly, since safety constraints for each CAV involve the trajectory of other CAVs, inspired by the idea of environmental CBFs [25], we consider the evolution of other relevant CAVs in constructing our CBFs. By introducing a barrier certificate as a safety middle layer between the vehicle-level tracking controller and physical vehicle, we provide a reactive mechanism to guarantee constraint satisfaction in the system.

This paper advances the state of the art in several ways. First, in contrast to other efforts which attempt to address

This research was supported by ARPAE's NEXTCAR program under the award number DE-AR0000796. This support is gratefully acknowledged.

B. Chalaki is with the Honda Research Institute, Ann Arbor, MI 48103, USA (email: behdad_chalaki@honda-ri.com)

A.A. Malikopoulos is with the Department of Mechanical Engineering, University of Delaware, Newark, DE 19716 USA (emails: andreas@udel.edu)

Authorized licensed use limited to: Cornell University Library. Downloaded on October 10,2023 at 15:11:35 UTC from IEEE Xplore. Restrictions apply.

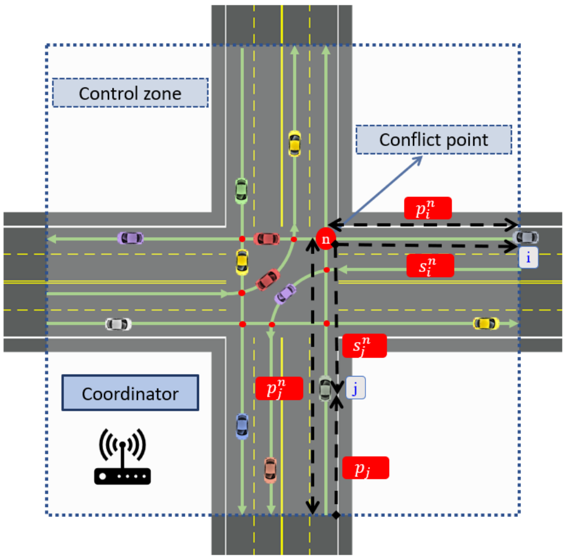

Fig. 1: A signal free intersection with conflict points.

satisfaction of all the constraints in the system through CBFs [19]–[22], in this paper, the motion planning module yields an optimal unconstrained trajectory which guarantees that state, control, and safety constraints are satisfied, while barrier-certificate module only intervenes if the deviations from the nominal optimal trajectory lead to violating the constraints. Second, in several research efforts using CBFs, the lateral safety is handled through imposing a FIFO queuing policy [18]–[21]. However, in our approach, we do not consider a FIFO queuing policy. Relaxing a FIFO queuing policy is not a trivial task since it introduces a constraint with higher relative degree, which requires special analysis.

The remainder of the paper is structured as follows. In Section II, we introduce the general modeling framework. In Section III, we present the motion planning, and in Section IV, we introduce the barrier-certificate modules. We provide simulation results in Section V, and concluding remarks in Section VI.

II. Modeling Framework

We consider a signal-free intersection (Fig. 1) which includes a *coordinator* that stores information about the intersection's geometry and CAVs' trajectories. The coordinator only acts as a database for the CAVs and does not make any decision. The intersection includes a *control zone* inside of which the CAVs can communicate with the coordinator. We call the points inside the control zone where paths of CAVs intersect and a lateral collision may occur as *conflict points*. Let $\mathcal{O} \subset \mathbb{N}$ be the set of conflict points, $N(t) \in \mathbb{N}$ be the total number of CAVs inside the control zone at time $t \in \mathbb{R}_{\geq 0}$, and $\mathcal{N}(t) = \{1, \dots, N(t)\}$ be the queue that designates the order in which each CAV entered the control zone.

Our coordination framework architecture consists of two main interconnected components called motion planning and barrier certificate. Using the simplified dynamics of each CAV, the motion planning module which is built based on the approach reported in [10] yields an optimal exit time from the control zone. The resulting optimal exit time corresponds to the unconstrained optimal control trajectory, derived using simple dynamics, and guarantees that none of the state, control, and safety constraints becomes active. The approach in [10] considers that a vehicle-level tracking controller can perfectly track the resulting optimal trajectory from the motion planning module. In this paper, however, we no longer consider this and introduce the vehicle-level tracking controller that employs a combined feedforward-feedback control law to track the resulting optimal trajectory from the motion planning module. Then, we introduce an intermediate barrier certificate module between the vehicle-level tracking controller and physical vehicle, which takes the reference control law, and by using complex vehicle dynamics, it ensures that none of the constraints in the system are violated.

III. Motion Planning

For the motion planning module, we model the dynamics of each CAV $i \in \mathcal{N}(t)$ as a double integrator

$$\dot{p}_i(t) = v_i(t), \quad \dot{v}_i(t) = u_i(t), \tag{1}$$

where $p_i(t) \in \mathcal{P}_i$, $v_i(t) \in \mathcal{V}_i$, and $u_i(t) \in \mathcal{U}_i$ denote position, speed, and control input at t, respectively. Let $t_i^0 \in \mathbb{R}_{\geq 0}$ be the time that CAV $i \in \mathcal{N}(t)$ enters the control zone, and $t_i^f \in \mathbb{R}_{\geq 0}$ be the time that CAV i exits the control zone. For each CAV $i \in \mathcal{N}(t)$, the control input and speed are bounded by

$$u_{i,\min} \leq u_i(t) \leq u_{i,\max}, \tag{2}$$

$$0 < v_{\min} \leq v_i(t) \leq v_{\max}, \tag{3}$$

where $u_{i,\min}, u_{i,\max}$ are the control bounds and $v_{\min}, v_{\max}$ are the minimum and maximum speed limits, respectively.

To guarantee rear-end safety between CAV $i \in \mathcal{N}(t)$ and a preceding CAV $k \in \mathcal{N}(t)$, we impose the following constraint,

$$p_k(t) - p_i(t) \geq \underbrace{\gamma + \varphi\, v_i(t)}_{\delta_i(t)}, \tag{4}$$

where $\delta_i(t)$ is the safe speed-dependent distance, while γ and $\varphi \in \mathbb{R}_{>0}$ are the standstill distance and reaction time, respectively.

Definition 1. *For CAV $i \in \mathcal{N}(t)$, and a conflict point $n \in \mathcal{O}$, $s_i^n : \mathbb{R}_{\geq 0} \to \mathbb{R}$ is the function that gives the distance between CAV i and conflict point n (Fig. 1), and it is given by*

$$s_i^n(t) = p_i^n - p_i(t), \quad \forall t \in [t_i^0, t_i^f], \tag{5}$$

where p_i^n is the distance of the conflict point $n \in \mathcal{O}$ from the point that CAV i enters the control zone.

Let CAV $j \in \mathcal{N}(t)$ be a CAV that has already planned its trajectory which might cause a lateral collision with CAV i. CAV i can reach at conflict point n either after or before CAV j. In the first case, we have

$$s_i^n(t) + s_j^n(t) \geq \delta_i(t), \quad \forall t \in [t_i^0, t_j^n], \tag{6}$$

Authorized licensed use limited to: Cornell University Library. Downloaded on October 10,2023 at 15:11:35 UTC from IEEE Xplore. Restrictions apply.

where t_j^n is the known time that CAV j reaches the conflict point n, i.e., position p_j^n. The intuition in (6) is that at t_j^n, s_j^n is equal to zero based on Definition 1, and CAV i should maintain at least a safe distance $\delta_i(t)$ from the conflict point n. However, for $t \in [t_i^0, t_j^n)$, s_j^n is a positive number, and hence $s_i^n(t)$ needs to be greater than $\delta_i(t) - s_j^n(t)$. Similarly, in the second case, where CAV i reaches the conflict point n before CAV j, we have

$$s_i^n(t) + s_j^n(t) \geq \delta_j(t), \quad \forall t \in [t_i^0, t_i^n], \tag{7}$$

where t_i^n is determined by the trajectory planned by CAV i.

Since $0 < v_{\min} \leq v_i(t)$, the position $p_i(t)$ is a strictly increasing function. Thus, the inverse $t_i(\cdot) = p_i^{-1}(\cdot)$ exists and it is called the *time trajectory* of CAV i [10]. Hence, we have $t_i^n = p_i^{-1}(p_i^n)$. Therefore, for each candidate path of CAV i, there exists a unique time trajectory which can be evaluated at conflict point n to find the time t_i^n that CAV i reaches at conflict point n.

However, to ensure the lateral safety between CAV i and CAV j at conflict point n, either (6) or (7) must be satisfied, and thus we impose the following lateral safety constraint on CAV i

$$\max\Bigg\{ \min_{t\in[t_i^0,t_j^n]} \{s_i^n(t) + s_j^n(t) - \delta_i(t)\}, \\ \min_{t\in[t_i^0,t_i^n]} \{s_i^n(t) + s_j^n(t) - \delta_j(t)\} \Bigg\} \geq 0. \tag{8}$$

Next, we briefly review the motion planning module that includes the single-level optimization framework for coordination of CAV reported in [10]. In this framework, each CAV i communicates with the coordinator to solve a time minimization problem, which determines t_i^f. This optimal exit time corresponds to the unconstrained optimal control trajectory which guarantees that none of the state, control, and safety constraints becomes active. This trajectory is communicated back to the coordinator, so that the subsequent CAVs receive this information and plan their trajectories accordingly. Using the unconstrained optimal control trajectory in $[t_i^0, t_i^f]$, we essentially avoid the inherent implementation challenges in solving a constrained optimal control in real time which requires piecing constrained and unconstrained arcs together [26], [27].

To formally define the motion planning problem, we first start with the unconstrained optimal control solution of CAV i, which has the following form [10]

$$u_i(t) = 6a_it + 2b_i, \quad v_i(t) = 3a_it^2 + 2b_it + c_i, \\ p_i(t) = a_it^3 + b_it^2 + c_it + d_i, \tag{9}$$

where a_i, b_i, c_i, and d_i are constants of integration. CAV i must also satisfy the boundary conditions

$$p_i(t_i^0) = 0, \quad v_i(t_i^0) = v_i^0, \tag{10}$$

$$p_i(t_i^f) = p_i^f, \quad u_i(t_i^f) = 0, \tag{11}$$

where $u_i(t_i^f) = 0$ because the speed at the exit of the control zone is not specified [28]. The details of the derivation of the unconstrained solution are discussed in [10].

Next, we formally define the motion planning problem to minimize the exit time from the control zone.

Problem 1. *Each CAV $i \in \mathcal{N}(t)$ solves the following optimization problem at t_i^0, upon entering the control zone*

$$\min_{t_i^f \in \mathcal{T}_i(t_i^0)} t_i^f \tag{12}$$

$$\text{subject to: (4), (8), (9), (10), (11),}$$

where the compact set $\mathcal{T}_i(t_i^0)$ is the set of feasible solution of CAV $i \in \mathcal{N}(t)$ for the exit time computed at t_i^0 using the speed and control input constraints (2)-(3), initial condition (10), and final condition (11). The derivation of this compact set is discussed in [27].

Solving Problem 1, CAV i derives the optimal exit time, t_i^f, corresponding to an optimal trajectory, $\bar{u}_i(t), \bar{v}_i(t)$ and $\bar{p}_i(t)$, which satisfies all the state, control, and safety constraints.

A vehicle-level tracking controller employs a combined feedforward-feedback control law u_i^{ref} to track the resulting optimal trajectory from the motion planning module as follows

$$u_i^{ref}(t) = \bar{u}_i(t) + k_p \cdot (\bar{p}_i(t) - p_i(t)) + k_v \cdot (\bar{v}_i(t) - v_i(t)), \tag{13}$$

where $p_i(t)$ and $v_i(t)$ are current observed position and speed of CAV i; respectively, while $k_p, k_v \in \mathbb{R}_{>0}$ are feedback control gains.

IV. Barrier-Certificate

In this section, we present our barrier-certificate module which is a middle layer between the vehicle-level tracking controller and physical vehicle. In this module, we consider more realistic model to describe the dynamics of each CAV $i \in \mathcal{N}(t)$ as follows

$$\dot{p}_i(t) = v_i(t), \quad \dot{v}_i(t) = u_i(t) - \frac{F_r(v_i(t))}{m_i}. \tag{14}$$

Let $F_r \in \mathbb{R}_{\geq 0}$ correspond to all resisting forces including longitudinal aerodynamic drag force and rolling resistance force at tires, while $m_i \in \mathbb{R}_{\geq 0}$ is the mass of CAV [29], [30]. The net resisting force typically is approximated as a quadratic function of the CAV's speed [29, Chapter 2], i.e.,

$$F_r(v_i(t)) = \beta_0 + \beta_1\, v_i(t) + \beta_2\, v_i^2(t), \tag{15}$$

where $\beta_0, \beta_1, \beta_2 \in \mathbb{R}_{\geq 0}$ are all constant parameters that can be computed empirically. We write (14) in a control-affine, vector form as

$$\dot{\mathbf{x}}_i(t) = \underbrace{\begin{bmatrix} v_i(t) \\ -\frac{F_r(v_i(t))}{m_i} \end{bmatrix}}_{\mathbf{f}_i(\mathbf{x}_i(t))} + \underbrace{\begin{bmatrix} 0 \\ 1 \end{bmatrix}}_{\mathbf{g}_i(\mathbf{x}_i(t))} u_i(t), \tag{16}$$

where $\mathbf{x}_i(t) = [p_i(t), v_i(t)]^\top \in \mathcal{P}_i \times \mathcal{V}_i$ denotes the state of the CAV i at t.

We first review some basic definitions and results from [16], [17] adapted appropriately to reflect our notation. Inspired by the idea of environmental CBFs [25], we construct

Authorized licensed use limited to: Cornell University Library. Downloaded on October 10,2023 at 15:11:35 UTC from IEEE Xplore. Restrictions apply.

a CBF for the cases in which the constraint of the CAV is coupled to the dynamics of other CAVs, such as lateral safety and rear-end safety constraints. To simplify notation, we discard the argument of time in our state and control variables whenever it does not create confusion.

Next, we define the safe set of a constraint that depends only on the state of a CAV.

Definition 2. *For CAV $i \in \mathcal{N}(t)$, the safe set $\mathcal{C}$ is a zero-superlevel set of a continuously differentiable function $h : \mathcal{P}_i \times \mathcal{V}_i \to \mathbb{R}$,*

$$\mathcal{C} = \{\mathbf{x}_i \in \mathcal{P}_i \times \mathcal{V}_i : h(\mathbf{x}_i) \geq 0\}. \quad (17)$$

For those cases where a constraint of CAV i depends also on another CAV j, i.e., in rear-end safety and lateral safety constraints, we define the coupled safe set next.

Definition 3. *For CAV $i \in \mathcal{N}(t)$, the coupled safe set $\mathcal{C}'$ with CAV $j \in \mathcal{N}(t)$ is a zero-superlevel set of a continuously differentiable function $z : D \subseteq (\mathcal{P}_i \times \mathcal{V}_i) \times (\mathcal{P}_j \times \mathcal{V}_j) \to \mathbb{R}$,*

$$\mathcal{C}' = \{(\mathbf{x}_i, \mathbf{x}_j) \in D : z(\mathbf{x}_i, \mathbf{x}_j) \geq 0\}. \quad (18)$$

Next, we define the safety of the CAV i, with longitudinal dynamics (16), with respect to the safe set $\mathcal{C}$ and coupled safe set $\mathcal{C}'$.

Definition 4. *CAV i with dynamics given by (16) is safe with respect to the safe set $\mathcal{C}$ if the set $\mathcal{C}$ is forward-invariant, namely, if $\mathbf{x}_i(t_i^0) \in \mathcal{C}$, $\mathbf{x}_i(t) \in \mathcal{C}$ for all $t \geq t_i^0$.*

Definition 5. *CAV i with dynamics given by (16) is safe with respect to the coupled safe set $\mathcal{C}'$ with CAV j, if the set $\mathcal{C}'$ is forward-invariant, namely, if $(\mathbf{x}_i(t_i^0), \mathbf{x}_j(t_i^0)) \in \mathcal{C}'$, $(\mathbf{x}_i(t), \mathbf{x}_j(t)) \in \mathcal{C}'$ for all $t \geq t_i^0$.*

We define the extended class $\mathcal{K}_\infty$ function as a strictly increasing function $\alpha : \mathbb{R} \to \mathbb{R}$ with $\alpha(0) = 0$.

Definition 6 ([16]). *Let $\mathcal{C}$ be a safe set for CAV $i \in \mathcal{N}(t)$ for a continuously differentiable function $h : \mathcal{P}_i \times \mathcal{V}_i \to \mathbb{R}$. The function h is a CBF if there exists an extended class $\mathcal{K}_\infty$ function $\alpha(\cdot)$ such that for all $\mathbf{x}_i \in \mathcal{C}$, $\sup_{u_i \in \mathcal{U}_i} \dot{h}(\mathbf{x}_i, u_i) \geq -\alpha(h(\mathbf{x}_i))$, where $\dot{h}(\mathbf{x}_i, u_i) = \nabla h(\mathbf{x}_i) \cdot \dot{\mathbf{x}}_i$ and $\dot{\mathbf{x}}_i$ is given by (16).*

Theorem 1 ([16]). *Let $\mathcal{C}$ be a safe set for CAV $i \in \mathcal{N}(t)$ for a continuously differentiable function $h : \mathcal{P}_i \times \mathcal{V}_i \to \mathbb{R}$. If h is a CBF on $\mathcal{P}_i \times \mathcal{V}_i$, then any Lipschitz continuous controller $u_i : \mathcal{P}_i \times \mathcal{V}_i \to \mathcal{U}_i$ such that $u_i(\mathbf{x}_i) \in \mathcal{A}_h(\mathbf{x}_i)$ renders the safe set $\mathcal{C}$ forward invariant, where*

$$\mathcal{A}_h(\mathbf{x}_i) = \{u_i \in \mathcal{U}_i : \nabla h(\mathbf{x}_i) \cdot \dot{\mathbf{x}}_i \geq -\alpha(h(\mathbf{x}_i))\}. \quad (19)$$

Inspired by the idea of environmental CBF [25], which considers the evolution of environment state in analyzing safety, we consider the evolution of other relevant CAVs in constructing the CBF for CAV i.

Definition 7. *Let $\mathcal{C}'$ be a coupled safe set for CAV i and $j \in \mathcal{N}(t)$ for a continuously differentiable function $z : D \subseteq (\mathcal{P}_i \times \mathcal{V}_i) \times (\mathcal{P}_j \times \mathcal{V}_j) \to \mathbb{R}$. The function z is a CBF if there exists an extended class $\mathcal{K}_\infty$ function $\alpha(\cdot)$ such that for all $(\mathbf{x}_i, \mathbf{x}_j) \in \mathcal{C}'$, $\sup_{u_i \in \mathcal{U}_i} \dot{z}(\mathbf{x}_i, u_i, \mathbf{x}_j, u_j) \geq -\alpha(z(\mathbf{x}_i, \mathbf{x}_j))$, where*

$$\begin{aligned}\dot{z}(\mathbf{x}_i, u_i, \mathbf{x}_j, u_j) = \nabla_{\mathbf{x}_i} z(\mathbf{x}_i, \mathbf{x}_j) \cdot \underbrace{(\mathbf{f}_i(\mathbf{x}_i) + \mathbf{g}_i(\mathbf{x}_i) u_i)}_{\dot{\mathbf{x}}_i} \\ + \nabla_{\mathbf{x}_j} z(\mathbf{x}_i, \mathbf{x}_j) \cdot \underbrace{(\mathbf{f}_j(\mathbf{x}_j) + \mathbf{g}_j(\mathbf{x}_j) u_j)}_{\dot{\mathbf{x}}_j},\end{aligned} \quad (20)$$

$$\nabla_{\mathbf{x}_i} z(\mathbf{x}_i, \mathbf{x}_j) = \left[\frac{\partial z(\mathbf{x}_i, \mathbf{x}_j)}{\partial p_i}, \frac{\partial z(\mathbf{x}_i, \mathbf{x}_j)}{\partial v_i}\right]^\top, \quad (21)$$

$$\nabla_{\mathbf{x}_j} z(\mathbf{x}_i, \mathbf{x}_j) = \left[\frac{\partial z(\mathbf{x}_i, \mathbf{x}_j)}{\partial p_j}, \frac{\partial z(\mathbf{x}_i, \mathbf{x}_j)}{\partial v_j}\right]^\top. \quad (22)$$

Theorem 2. *Let $\mathcal{C}'$ be a coupled safe set for CAV $i \in \mathcal{N}(t)$ and $j \in \mathcal{N}(t)$ for a continuously differentiable function $z : D \subseteq (\mathcal{P}_i \times \mathcal{V}_i) \times (\mathcal{P}_j \times \mathcal{V}_j) \to \mathbb{R}$. If z is a CBF on D, then any Lipschitz continuous controller $u_i : D \to \mathcal{U}_i$ such that $u_i(\mathbf{x}_i, \mathbf{x}_j) \in \mathcal{A}_z(\mathbf{x}_i, \mathbf{x}_j)$ renders the coupled safe set $\mathcal{C}'$ forward invariant, where*

$$\begin{aligned}\mathcal{A}_z(\mathbf{x}_i, \mathbf{x}_j) = \{u_i \in \mathcal{U}_i : \nabla_{\mathbf{x}_i} z(\mathbf{x}_i, \mathbf{x}_j) \cdot \dot{\mathbf{x}}_i \\ + \nabla_{\mathbf{x}_j} z(\mathbf{x}_i, \mathbf{x}_j) \cdot \dot{\mathbf{x}}_j \geq -\alpha(z(\mathbf{x}_i, \mathbf{x}_j))\}.\end{aligned} \quad (23)$$

Proof. The proof is similar to the one in [25, Theorem 2], and thus is omitted. □

Next, we construct CBFs for (3)-(7). For the speed constraint (3) of CAV i, we consider $h_1(\mathbf{x}_i) = v_{\max} - v_i$, $h_2(\mathbf{x}_i) = v_i - v_{\min}$. From Definition 6 and choosing $\alpha_q(x) = \lambda_q x$, $\lambda_q \in \mathbb{R}_{>0}, q \in \{1, 2\}$, we have $h_1(\mathbf{x}_i)$ and $h_2(\mathbf{x}_i)$ as CBFs to ensure satisfying the speed limit constraint. Then, from Theorem 1, any control input u_i should satisfy the following

$$u_i \leq \frac{F_r(v_i)}{m_i} + \lambda_1(v_{\max} - v_i), \quad (24)$$

$$u_i \geq \frac{F_r(v_i)}{m_i} - \lambda_2(v_i - v_{\min}). \quad (25)$$

Since rear-end safety constraint depends on both states of CAV i and $k \in \mathcal{N}(t)$, we have $z_1(\mathbf{x}_i, \mathbf{x}_k) = p_k - p_i - (\gamma + \varphi \cdot v_i)$. From Definition 7 and choosing $\alpha_3(x) = \lambda_3 x$, $\lambda_3 \in \mathbb{R}_{>0}$, we have $z_1(\mathbf{x}_i, \mathbf{x}_k)$ as a CBF to guarantee satisfying the rear-end safety constraint. Using the result of Theorem 2, the control input u_i should satisfy the following condition in order to satisfy the rear-end safety constraint,

$$u_i \leq \frac{1}{\varphi}\left[\lambda_3(p_k - p_i - (\gamma + \varphi v_i)) + v_k - v_i\right] + \frac{F_r(v_i)}{m_i}. \quad (26)$$

For the lateral-safety constraint (6), when $t_i^n > t_j^n$, we have $z_2(\mathbf{x}_i, \mathbf{x}_j) = s_i^n + s_j^n - \delta_i = (p_i^n - p_i) + (p_j^n - p_j) - (\gamma + \varphi \cdot v_i)$. By choosing $\alpha_4(x) = \lambda_4 x$, $\lambda_4 \in \mathbb{R}_{>0}$, $z_2(\mathbf{x}_i, \mathbf{x}_j)$ is a CBF to guarantee satisfying the lateral safety constraint. For this case, the control input u_i should satisfy the following condition in order to satisfy constraint (6),

$$u_i \leq \frac{1}{\varphi}\left[\lambda_4(s_i^n + s_j^n - \delta_i) - (v_i + v_j)\right] + \frac{F_r(v_i)}{m_i}. \quad (27)$$

Authorized licensed use limited to: Cornell University Library. Downloaded on October 10,2023 at 15:11:35 UTC from IEEE Xplore. Restrictions apply.

For the lateral-safety constraint (7), we have

$$z_3(\mathbf{x}_i, \mathbf{x}_j) = s_i^n + s_j^n - \delta_j. \tag{28}$$

However, since $\dot{z}_3$ does not depend on u_i, (28) cannot be a valid CBF for CAV i. These type of constraints are called constraints with higher relative degree $r > 1$. For example, the relative degree of (7) is equal to 2. A complete analysis of handling higher relative degree constraints in general cases is given in [31].

Next, we use a higher order CBF based on [31, Definition 7, Theorem 5], and extend it to our case with coupled constraints. We first form a series of functions $\psi_q : D \subseteq (\mathcal{P}_i \times \mathcal{V}_i) \times (\mathcal{P}_j \times \mathcal{V}_j) \to \mathbb{R}$, $q = \{0, 1, 2\}$ as

$$\begin{aligned} \psi_0(\mathbf{x}_i, \mathbf{x}_j) &= z_3(\mathbf{x}_i, \mathbf{x}_j), \\ \psi_1(\mathbf{x}_i, \mathbf{x}_j) &= \dot{\psi}_0(\mathbf{x}_i, \mathbf{x}_j) + \alpha_5(\psi_0(\mathbf{x}_i, \mathbf{x}_j)), \\ \psi_2(\mathbf{x}_i, \mathbf{x}_j) &= \dot{\psi}_1(\mathbf{x}_i, \mathbf{x}_j) + \alpha_6(\psi_1(\mathbf{x}_i, \mathbf{x}_j)), \end{aligned} \tag{29}$$

where $\alpha_5(\cdot)$ and $\alpha_6(\cdot)$ are extended class $\mathcal{K}_\infty$ functions. The zero-superlevel sets of ψ_0 and ψ_1 are given by $\mathcal{C}_1' = \{(\mathbf{x}_i, \mathbf{x}_j) \in D : \psi_0(\mathbf{x}_i, \mathbf{x}_j) \geq 0\}$, $\mathcal{C}_2' = \{(\mathbf{x}_i, \mathbf{x}_j) \in D : \psi_1(\mathbf{x}_i, \mathbf{x}_j) \geq 0\}$. Based on [31, Definition 7], if there exist extended class $\mathcal{K}_\infty$ functions $\alpha_5(\cdot)$ and $\alpha_6(\cdot)$ such that $\psi_2(\mathbf{x}_i, \mathbf{x}_j) \geq 0$ for all $(\mathbf{x}_i, \mathbf{x}_j) \in \mathcal{C}_1' \cap \mathcal{C}_2'$, $z_3(\mathbf{x}_i, \mathbf{x}_j)$ is a higher order CBF. From [31, Theorem 5], if $(\mathbf{x}_i(t_i^0), \mathbf{x}_j(t_i^0)) \in \mathcal{C}_1' \cap \mathcal{C}_2'$, then any Lipschitz continuous controller $u_i : D \to \mathbb{R}$ such that $u_i(\mathbf{x}_i, \mathbf{x}_j) \in \mathcal{A}_\psi(\mathbf{x}_i, \mathbf{x}_j)$ renders the set $\mathcal{C}_1' \cap \mathcal{C}_2'$ forward invariant, where

$$\mathcal{A}_\psi(\mathbf{x}_i, \mathbf{x}_j) = \{u_i \in \mathcal{U}_i : \psi_2(\mathbf{x}_i, \mathbf{x}_j) \geq 0\}. \tag{30}$$

Theorem 3. *The allowable set of control actions that renders the set $\mathcal{C}_1' \cap \mathcal{C}_2'$ forward invariant, $\mathcal{A}_\psi$, is given by*

$$\begin{aligned} u_i \leq & -\lambda_5(v_i + v_j) + \frac{F_r(v_i)}{m_i} + \frac{F_r(v_j)}{m_j} - \frac{\varphi\beta_1 F_r(v_j)}{m_j^2} \\ & - \frac{2\varphi\beta_2 v_j F_r(v_j)}{m_j^2} + (\frac{\varphi\beta_1 + 2\varphi\beta_2 v_j}{m_j} - \lambda_5\varphi - 1)u_j \\ & - \varphi\dot{u}_j + \lambda_6\ \psi_1. \end{aligned} \tag{31}$$

Proof. Due to the lack of space, the proof is omitted and can be found in the longer version of the paper [32].

□

Depending on the the arrival time at conflict point n for CAV i and j (t_i^n and t_j^n, respectively), we must satisfy (27) or (31) as follows

$$\begin{cases} u_i \leq A, & \text{if } t_i^n > t_j^n \\ u_i \leq B, & \text{if } t_i^n < t_j^n \end{cases}, \tag{32}$$

where

$$A = \frac{1}{\varphi}\left[\lambda_4(s_i^n + s_j^n - \delta_i) - (v_i + v_j)\right] + \frac{F_r(v_i)}{m_i}, \tag{33}$$

$$\begin{aligned} B = & \lambda_5(v_i + v_j) + \frac{F_r(v_i)}{m_i} + \frac{F_r(v_j)}{m_j} - \frac{\varphi\beta_1 F_r(v_j)}{m_j^2} \\ & - \frac{2\varphi\beta_2 v_j F_r(v_j)}{m_j^2} + (\frac{\varphi\beta_1 + 2\varphi\beta_2 v_j}{m_j} - \lambda_5\varphi - 1)u_j \\ & - \varphi\dot{u}_j + \lambda_6\ \psi_1. \end{aligned} \tag{34}$$

Next, we formulate an optimization problem based on QP for our barrier-certificate module. This QP can be solved at discrete time step to verify the reference control input $u_i^{ref}(t)$, resulting from the vehicle-level tracking controller. In case of a potential violation, QP minimally modifies the control input to guarantee the satisfaction of all constraints.

Problem 2. *Each CAV $i \in \mathcal{N}(t)$ at time t observes its state $\mathbf{x}_i$ and accesses the states and control inputs, $\mathbf{x}_j$ and u_j, respectively, of neighbour CAVs. Then, i solves the following optimization problem to find the safe control input.*

$$u_i^*(t) = \underset{u_i(t)}{\arg\min}\ \frac{1}{2}\|u_i(t) - u_i^{ref}(t)\|^2 \tag{35}$$

subject to:

(2), (24), (25), (26), (32),

where each pertaining constraint (3)-(7) for CAV i are mapped to the control input constraint using the appropriate CBFs (19), (23), or (30). Note that $u_i^{ref}(t)$ is the combined feedforward-feedback control law to track the resulting optimal trajectory from the motion planning module III.

Since the control input is bounded, the feasibility of the QP in Problem 2 can be ensured by choosing appropriate $\lambda_q \in \mathbb{R}_{\geq 0}$ for class $\mathcal{K}_\infty$ functions $\alpha_q(x) = \lambda_q x$, $q \in \mathbb{N}$. Note that in this paper, we chose linear class $\mathcal{K}_\infty$ functions; however, one may decide to choose a different form for their class $\mathcal{K}_\infty$. Analyzing the effects of the choice of $\mathcal{K}_\infty$ on the control input's feasible space is left for future work.

V. Simulation Results

To show the performance of our framework, we investigate the coordination of 24 CAVs at a signal-free intersection shown in Fig.1. The CAVs enter the control zone from 6 different paths (Fig. 1) with a total rate of 3600 veh/hour while their initial speed is uniformly distributed between 12 m/s and 14 m/s. We consider the length of the control zone and road width to be 212 m and 3 m, respectively. The rest of the parameters for the simulation are $v_{\min} = 0.2$ m/s, $v_{\max} = 20$ m/s, $u_{\max} = 2$ m/s^2, $u_{\min} = -2$ m/s^2, $\gamma = 2.5$ m, $\varphi = 0.5$ s $k_p = k_v = 1.5$, $\Delta t = 0.1$ s. We used `lsqlin` in Matlab to solve Problem 2 and `ODE45` to integrate the vehicle dynamics. Videos from our simulation can be found at the supplemental site, https://sites.google.com/view/ud-ids-lab/BCOCF.

Figs. 2 demonstrates the control input for a selected CAV in the simulation. The blue line in Fig. 2 shows the reference control input from the feedforward-feedback control law (13), and the dashed red line denotes the resulting optimal control trajectory from the motion planning module. The black line shows the applied control input at each time step resulting from the Solution of Problem 2. It can be seen that around 16.5 s the barrier-certificate module overrides the reference control input in order to satisfy the speed limit constraint. Moreover, the mean and standard deviation of computation times for the motion planning module are 0.029 s and 0.0331 s; respectively, and for barrier-certificate module are 0.0063 s and 0.0026 s, respectively.

Authorized licensed use limited to: Cornell University Library. Downloaded on October 10,2023 at 15:11:35 UTC from IEEE Xplore. Restrictions apply.

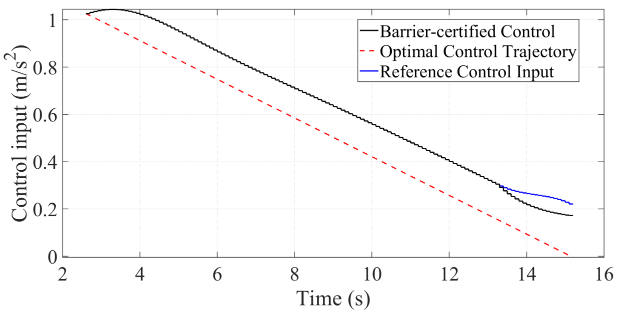

Fig. 2: Control input for a selected CAV.

VI. Concluding Remarks and Discussion

In this paper, we enhanced the motion planning framework for coordination of CAVs introduced in [10] through employing CBFs to provide an additional safety layer and ensure satisfaction of all constraints in the system. In the motion planning module, each CAV first uses simple longitudinal dynamics to derive the optimal control trajectory without activating any constraint. In a real physical system, we require a vehicle-level controller to track the resulting optimal trajectory. However, due to the inherent deviations between the actual trajectory and the planned trajectory, the system's constraints may become active. We addressed this issue by introducing a barrier-certificate module based on a more realistic dynamics as a safety middle layer between the vehicle-level tracking controller and physical vehicle to provide a reactive mechanism to guarantee constraint satisfaction in the system. Future work should validate this framework beyond simulation using a physical system.

References

[1] M. Athans, "A unified approach to the vehicle-merging problem," *Transportation Research*, vol. 3, no. 1, pp. 123–133, 1969.

[2] H. Xu, Y. Zhang, L. Li, and W. Li, "Cooperative driving at unsignalized intersections using tree search," *IEEE Transactions on Intelligent Transportation Systems*, vol. 21, no. 11, pp. 4563–4571, 2019.

[3] H. Xu, Y. Zhang, C. G. Cassandras, L. Li, and S. Feng, "A bi-level cooperative driving strategy allowing lane changes," *Transportation research part C: emerging technologies*, vol. 120, p. 102773, 2020.

[4] M. A. Guney and I. A. Raptis, "Scheduling-based optimization for motion coordination of autonomous vehicles at multilane intersections," *Journal of Robotics*, vol. 2020, 2020.

[5] R. Hult, M. Zanon, S. Gros, and P. Falcone, "Optimal coordination of automated vehicles at intersections: Theory and experiments," *IEEE Transactions on Control Systems Technology*, vol. 27, no. 6, pp. 2510–2525, 2018.

[6] B. Chalaki and A. A. Malikopoulos, "Time-optimal coordination for connected and automated vehicles at adjacent intersections," *IEEE Transactions on Intelligent Transportation Systems*, 2021.

[7] S. A. Fayazi and A. Vahidi, "Mixed-integer linear programming for optimal scheduling of autonomous vehicle intersection crossing," *IEEE Transactions on Intelligent Vehicles*, vol. 3, no. 3, pp. 287–299, 2018.

[8] B. Chalaki and A. A. Malikopoulos, "Optimal control of connected and automated vehicles at multiple adjacent intersections," *IEEE Transactions on Control Systems Technology*, vol. 30, no. 3, pp. 972–984, 2022.

[9] A. I. Mahbub, A. A. Malikopoulos, and L. Zhao, "Decentralized optimal coordination of connected and automated vehicles for multiple traffic scenarios," *Automatica*, vol. 117, no. 108958, 2020.

[10] A. A. Malikopoulos, L. E. Beaver, and I. V. Chremos, "Optimal time trajectory and coordination for connected and automated vehicles," *Automatica*, vol. 125, no. 109469, 2021.

[11] Y. Zhang and C. G. Cassandras, "Decentralized optimal control of connected automated vehicles at signal-free intersections including comfort-constrained turns and safety guarantees," *Automatica*, vol. 109, p. 108563, 2019.

[12] S. Kumaravel, A. A. Malikopoulos, and R. Ayyagari, "Optimal coordination of platoons of connected and automated vehicles at signal-free intersections," *IEEE Transactions on Intelligent Vehicles*, vol. 7, no. 2, pp. 186—197, 2022.

[13] K.-D. Kim and P. R. Kumar, "An MPC-based approach to provable system-wide safety and liveness of autonomous ground traffic," *IEEE Transactions on Automatic Control*, vol. 59, no. 12, pp. 3341–3356, 2014.

[14] G. R. Campos, P. Falcone, H. Wymeersch, R. Hult, and J. Sjöberg, "Cooperative receding horizon conflict resolution at traffic intersections," in *53rd IEEE Conference on Decision and Control*. IEEE, 2014, pp. 2932–2937.

[15] M. Kloock, P. Scheffe, S. Marquardt, J. Maczijewski, B. Alrifaee, and S. Kowalewski, "Distributed model predictive intersection control of multiple vehicles," in *2019 IEEE Intelligent Transportation Systems Conference (ITSC)*. IEEE, 2019, pp. 1735–1740.

[16] A. D. Ames, X. Xu, J. W. Grizzle, and P. Tabuada, "Control barrier function based quadratic programs for safety critical systems," *IEEE Transactions on Automatic Control*, vol. 62, no. 8, pp. 3861–3876, 2016.

[17] A. D. Ames, S. Coogan, M. Egerstedt, G. Notomista, K. Sreenath, and P. Tabuada, "Control barrier functions: Theory and applications," in *2019 18th European control conference (ECC)*. IEEE, 2019, pp. 3420–3431.

[18] W. Xiao, C. G. Cassandras, and C. A. Belta, "Bridging the gap between optimal trajectory planning and safety-critical control with applications to autonomous vehicles," *Automatica*, vol. 129, p. 109592, 2021.

[19] W. Xiao, C. Belta, and C. G. Cassandras, "Decentralized merging control in traffic networks: A control barrier function approach," in *Proceedings of the 10th ACM/IEEE International Conference on Cyber-Physical Systems*, 2019, pp. 270–279.

[20] M. Rodriguez and H. Fathy, "Vehicle and traffic light control through gradient-based coordination and control barrier function safety regulation," *Journal of Dynamic Systems, Measurement, and Control*, vol. 144, no. 1, 2022.

[21] S. Khaled, O. M. Shehata, and E. I. Morgan, "Intersection control for autonomous vehicles using control barrier function approach," in *2020 2nd Novel Intelligent and Leading Emerging Sciences Conference (NILES)*. IEEE, 2020, pp. 479–485.

[22] A. Katriniok, "Control-sharing control barrier functions for intersection automation under input constraints," *arXiv preprint arXiv:2111.10205*, 2021.

[23] B. Chalaki and A. A. Malikopoulos, "A priority-aware replanning and resequencing framework for coordination of connected and automated vehicles," *IEEE Control Systems Letters*, vol. 6, pp. 1772–1777, 2022.

[24] ——, "Robust learning-based trajectory planning for emerging mobility systems," in *2022 American Control Conference (ACC)*, 2022, pp. 2154–2159.

[25] T. G. Molnar, A. K. Kiss, A. D. Ames, and G. Orosz, "Safety-critical control with input delay in dynamic environment," *arXiv preprint arXiv:2112.08445*, 2021.

[26] A. M. I. Mahbub and A. A. Malikopoulos, "Conditions to Provable System-Wide Optimal Coordination of Connected and Automated Vehicles," *Automatica*, vol. 131, no. 109751, 2021.

[27] B. Chalaki, L. E. Beaver, and A. A. Malikopoulos, "Experimental validation of a real-time optimal controller for coordination of cavs in a multi-lane roundabout," in *31st IEEE Intelligent Vehicles Symposium (IV)*, 2020, pp. 504–509.

[28] A. E. Bryson and Y. C. Ho, *Applied optimal control: optimization, estimation and control*. CRC Press, 1975.

[29] H. K. Khalil, "Nonlinear systems third edition," *Patience Hall*, vol. 115, 2002.

[30] R. Rajamani, *Vehicle dynamics and control*. Springer Science & Business Media, 2011.

[31] W. Xiao and C. Belta, "Control barrier functions for systems with high relative degree," in *2019 IEEE 58th conference on decision and control (CDC)*. IEEE, 2019, pp. 474–479.

[32] B. Chalaki and A. A. Malikopoulos, "A Barrier-Certified Optimal Coordination Framework for Connected and Automated Vehicles," *Proceedings of the 61th IEEE Conference on Decision and Control (CDC), arXiv:2203.16418*, 2022 (to appear).

Authorized licensed use limited to: Cornell University Library. Downloaded on October 10,2023 at 15:11:35 UTC from IEEE Xplore. Restrictions apply.